Insights into structural features determining odorant affinities to honey bee odorant-binding protein 14

Andreas Schwaighofer[a], Maria Pechlaner[b], Chris Oostenbrink[b], Caroline Kotlowski[c], Can Araman[d], Rosa Mastrogiacomo[e], Paolo Pelosi[e], Wolfgang Knoll[a], Christoph Nowak[a,c,*] and Melanie Larisika[a,*]

[a]Austrian Institute of Technology GmbH, AIT, Donau-City Str. 1, 1220 Vienna, Austria

[b]Institute of Molecular Modeling and Simulation, University of Natural Resources and Life Sciences, Muthgasse 18, 1190 Vienna, Austria

[c]Center of Electrochemical Surface Technology, CEST, Viktor-Kaplan-Straße 2, 2700 Wiener Neustadt, Austria

[d]Institut für Biologische Chemie, Universität Wien, Währinger Straße 38, 1090 Wien, Austria

[e]Department of Agriculture, Food and Environment, University of Pisa, Via del Borghetto 80, 56124 Pisa, Italy

© 2019. This is the peer reviewed version of the following article: A. Schwaighofer, M. Pechlaner, C. Oostenbrink, C. Kotlowski, C. Araman, R. Mastrogiacomo, P. Pelosi, W. Knoll, C. Nowak, M. Larisika, Insights into structural features determining odorant affinities to honey bee odorant binding protein 14, Biochemical and biophysical research communications 446 (2014) 1042-1046, which has been published in final form at https://doi.org/10.1016/j.bbrc.2014.03.054. This manuscript version is made available under the CC-BY-NC-ND 4.0 license http://creativecommons.org/licenses/by-nc-nd/4.0/

Abstract

Molecular interactions between odorants and odorant binding proteins (OBPs) are of major importance for understanding the principles of selectivity of OBPs towards the wide range of semiochemicals. It is largely unknown on a structural basis, how an OBP binds and discriminates between odorant molecules. Here we examine this aspect in greater detail by comparing the C-minus OBP14 of the honey bee (*Apis mellifera* L.) to a mutant form of the protein that comprises the third disulfide bond lacking in C-minus OBPs. Affinities of structurally analogous odorants featuring an aromatic phenol group with different side chains were assessed based on changes of the thermal stability of the protein upon odorant binding monitored by circular dichroism spectroscopy. Our results indicate a tendency that odorants show higher affinity to the wild-type OBP suggesting that the introduced rigidity in the mutant protein has a negative effect on odorant binding. Furthermore, we show that OBP14 stability is very sensitive to the position and type of functional groups in the odorant.

Keywords

Odorant binding protein; circular dichroism; thermal stability; ligand binding; molecular dynamics

Introduction

Odorant binding proteins (OBPs) attracted increasing attention in recent years due to their potential application as biosensing elements for the fabrication of odorant sensors based on the olfactory system [1-4]. Applications are diverse and include disease diagnostics [5], food safety [6], and environmental monitoring [7]. These biomimetic sensor platforms potentially provide higher sensitivity combined with lower detection limits and faster response time compared to odorant sensors based on metal oxides and conducting polymers [8-10].

OBPs are abundant small proteins (~13-16 kDa) found in the olfactory epithelium of vertebrates and the sensillar lymph of insects [11]. The functional role of OBPs in olfaction is not fully resolved yet. However, high concentrations (10 mM) of OBPs in olfactory dendrites and the relatively high number of OBPs in the genome indicate important contributions [12,13]. A meanwhile widely accepted hypothesis describes OBPs as a carrier for hydrophobic odorant molecules through the sensillar lymph to the membrane which holds the odorant receptor cells [12,14].

The focus of this work is OBP14 of the honey bee (*Apis mellifera* L.). Investigation of the olfactory system in honey bees is of particular interest due to the high complexity of the chemical language used by these social insects to communicate among the members of the bee hive [15]. The genome of the honey bee comprises 21 OBPs [16], 13 of which are classified as classic OBPs (OBP1-13) and seven as C-minus OBPs with four Cys residues (OBP15-21). OBP14, also a member of the C-minus class, is unique, featuring five cysteines. It has been identified in different tissues of adult bees, as well as in larvae [17]. OBP14 exhibits 119 amino acid residues with a molecular weight of 13.5 kDa [18]. Typical for insect OBPs, its three dimensional structure predominantly consists of α-helical domains arranged in a very compact and stable structure, as depicted in Fig. 1A. Featuring five cysteines, OBP14

exhibits two disulfide bonds between residues 17(α1)-49(α3) and 88(α5)-106(α6) as well as an unpaired cysteine at position 47(α3) [18]. For investigation of the functional implications arising from structural differences between classic and C-minus OBPs, a double mutant Q44C-H97C of OBP14 was employed in this study, which comprises the third disulfide bond present in classical OBPs (see Fig. 1B) [18].

Ligand-binding characteristics and affinities of a wide range of odorants to OBPs of various species have been the subject of intensive research [19-21]. Typically, fluorescence binding studies are employed to indirectly determine the affinity of an odorant relative to a fluorescence reporter molecule [17,18,22,23]. Most recently, our lab presented a method of estimating odorant affinities to OBPs by monitoring the changes of thermal stability of the protein upon odorant binding by circular dichroism (CD) spectroscopy. This approach has been successfully applied to OBP14 and has been validated by infrared (IR) spectroscopy [24]. By evaluation of the different transition temperatures of geraniol and eugenol, it was possible to distinguish between the affinities of the two ligands. CD is a convenient method for studying the structure of proteins in solution and is particularly applicable to monitor dynamic changes in the secondary structure triggered by an external perturbation such as a temperature increase [25].

Increased protein stability upon ligand binding has been observed for a wide variety of biological systems [26-28]. Weak non-covalent forces such as hydrogen bonds as well as electrostatic, hydrophobic and aromatic interactions have been recognized to play a significant role in increasing the structural stability of the protein-ligand complexes [29-31]

In this work, we systematically analyze and evaluate structural parameters that influence an odorant's affinity to OBP14. So far, this has only been accomplished for odorant receptors [32,33]. However, with the growing interest in OBPs and their crucial role in olfaction, structural properties of their binding cavity are the consequential target of future

investigations. To address this question, we employed CD spectroscopy to compare the effect of ligand binding on the thermal stability of wild-type and mutant OBP14 and correlate the increase of stability with odorant affinity. The tested odorants include eugenol and its structural analogues, which belong to the family of phenyl propanoids, a group of compounds known for their role as semiochemicals for many insects [34]. Comparison of the wild-type and a mutant form of OBP14 reveals the impact of protein flexibility on the OBP's ability to adapt its binding cavity to fit different odorants with varying functional groups.

Materials and methods

Materials. Eugenol (4-Prop-2-enyl-2-methoxyphenol, 99%), Methyl eugenol (4-Allyl-1,2-dimethoxybenzene, 98%), 4-Vinylguaiacol (2-Methoxy-4-vinylphenol, 98%), Homovanillic acid (2-(4-Hydroxy-3-methoxy-phenyl)acetic acid, 98%), Coniferyl aldehyde (3-(4-hydroxy-3-methoxyphenyl)prop-2-enal, 98%), Coniferyl alcohol (4-(3-hydroxy-1-propenyl)-2-methoxyphenol, 98 %), Isoeugenol (2-methoxy-4-(prop-1-en-1-yl)phenol, 98%), Dihydroeugenol (2-Methoxy-4-propylphenol, 99%), 3,4-Dimethoxystyrene (techn.) were provided by Sigma-Aldrich (Steinheim, Germany).

Expression and purification of OBP14. Expression of recombinant proteins was done as described in Spinelli et al. [18]. Bacterial expression was performed along with established protocols [17,35] and purification was accomplished using conventional chromatographic techniques [36,37]. The purity of the protein was checked by SDS-PAGE.

Circular Dichroism. Far UV (260-195 nm) CD measurements were carried out using an Applied Photophysics Chirascan plus spectrophotometer (Leatherhead, Surrey, United Kingdom) equipped with a temperature control unit (Quantum TC125) in a 1 mm quartz cell at 1 nm resolution. Protein solutions (0.5 mg/mL; 41.8 μM) were prepared in phosphate buffer (140 mM NaCl, 3 mM KCl, 10 mM Na_2HPO_4, 2 mM KH_2PO_4, pH 8). For static measurements, ten spectra with the acquisition time of 0.5 s were taken at room temperature and the results were averaged. For measurement of OBP14 in the presence of odorants, the protein was incubated in solution with 200 μM odorant for 1 h. For temperature-controlled experiments, two acquisition techniques were employed. In spectra-kinetic mode, spectra were taken in the range of 20-90 °C (ΔT=5 °C) with an acquisition time of 0.2 s after an equilibration time of 45 s at each temperature step. In the kinetic mode, the ellipticity was recorded at a fixed wavelength of 222 nm with an acquisition time of 0.5 s.

MD simulations. MD simulations were performed using the GROMOS11 package for biomolecular simulations [38] and the GROMOS forcefield 54A8 [39] starting from the native and mutant OBP14 crystal structures (PDB ID: 3S0A and 3S0G) [18].Three 50-ns simulations each were performed at 300, 340, 360, 370 and 400 K. Detailed simulation settings are provided in the Supporting Information.

Results and discussion

Thermal stability of wild-type and mutant OBP14

Circular dichroism measurements of wild-type and mutant OBP14 at room temperature are shown in Fig. S1. The negative peak at 208 nm and the negative shoulder at 222 nm are a

clear indication for the high α-helical content of the proteins [40,41]. This secondary structure assignment is in agreement with X-ray diffraction and IR-spectroscopy [24].

Effects of the additional disulfide bond introduced to the protein on thermal stability of OBP14 were investigated by acquiring CD spectra while increasing the temperature between 20 and 90 °C in 5°C steps. Thermal denaturation of the proteins was followed by evaluation of the CD signal at 222 nm, which has been reported to be particularly sensitive to changes of the secondary structure [25,42]. Fig. S2 shows the ellipticity at 222 nm plotted versus temperature. The data points were fitted with a Boltzmann function for sigmoidal line shapes. The points of inflection, i.e., the temperature of maximum change for wild-type and mutant OBP14 are 56.6 and 64.9 °C, respectively. The transition temperature of wild-type OBP14 agrees well with the one reported for OBP14 (55.3 °C) in a previous study [24]. As expected, the transition temperature is higher for mutant OBP14 due to the introduced third disulfide bond that confers additional constraints in flexibility to the structure, thus preventing thermal denaturation [43]. MD simulations confirm a higher stability of the mutant as observed by the secondary structure content and atom-positional root-mean-square deviations from the X-ray structures (Fig. S3). Stabilization of proteins by disulfide bonds has been attributed to a decrease of conformational entropy [44]. Disulfide bonds form a covalent link between secondary structure elements and consequently increase protein thermostability by preventing the formation of incorrectly folded structures [45]. Consequently, an increase of thermal stability has been observed for many biological systems [46-48], most notably it was found that removal of a native disulfide bond in porcine OBP results in a decrease of the transition temperature of more than 30 °C [49].

Effect of functional group variation on odorant affinity

Odorant binding does not affect the structure of OBPs to a degree that can be monitored with instrumental techniques that detect alterations in the overall secondary structure, such as IR or CD spectroscopy [24,50,51]. Thus, changes in thermal stability of the protein upon odorant binding were assessed to estimate odorant affinities.

Effects on thermal stability of wild-type and mutant OBP14 due to odorant binding were studied by acquiring CD spectra while increasing the temperature between 20 and 90 °C in 5°C steps (exemplary spectra shown in Figs. S4-5). Control measurements of the buffer and odorant solutions without protein do not show any changes with increasing temperatures (Fig. S6). Thermal denaturation of the protein was evaluated by plotting the CD signal at 222 nm versus temperature. Fig. 2 shows the transition curves of the (A) wild-type and (B) mutant OBP14 in absence and presence of the investigated odorants. By applying a Boltzmann fit for sigmoidal lineshapes, the points of inflection were determined (temperatures indicated by arrows). The results are collected in Table S1. In Fig. 3, the change in transition temperature of the protein-ligand complex is shown relative to the transition temperature of the proteins in absence of odorants.

Consistent with earlier studies, the extent of temperature increase due to ligand binding is correlated with the affinity of the examined odorants [24,51].

In this study, odorants with a phenolic ring structure were systematically investigated, with a methoxy group as the R_3 substituent and variations at the R_1 and R_4 substituents on the benzene ring. Changes of the transition temperature due to ligand binding as represented in Fig. 3 allow identifying trends of odorant affinity associated with the different side groups that will be discussed in the following part. For the wild-type protein, eugenol (1), isoeugenol (3) and 4-vinylguaiacol (4) exhibit the highest observed affinities as measured by the

increasing thermal stability due to odorant binding. The high affinity of this odorant to wild-type OBP14 has been confirmed with a graphene-based FET sensor [4] in our lab as well as with fluorescence binding studies [17,18]. Out of the odorants listed above, eugenol shows a comparable affinity to mutant OBP14. Common structural features of these odorants are the hydroxyl group as R_4 and a hydrophobic chain as R_1. Strong hydrogen bonds between the hydroxyl group and adjacent amino acid residues in a particularly favorable tetrahedral geometry have been identified to play an important role in this strong binding [18].

Compared to odorants 1 and 4, in methyl eugenol (2) and 3,4-dimethoxystyrene (5) the hydroxyl group is exchanged with a methoxy group, while exhibiting the same functional group as R_1. Thus, the influence of the hydroxyl group on the affinity is directly experimentally observable. In the presence of the methoxy group, affinities to the wild-type protein decrease drastically with an additional decline for mutant OBP14. These results confirm the importance of the hydroxyl group to the protein-ligand interaction, as explained above.

For further investigations, the functionalities of the R_1 group were varied. Compounds 4 and 5 have a vinyl side chain, whereas odorants 1 and 2 exhibit an allyl side group. Particularly intriguing is the case of isoeugenol (3), which is a structural isomer of eugenol with the double bond in R_1 shifted from the second to the first carbon of the side chain. This means, the two molecules have the same size, but the location of the double bond is different. As shown in Fig. 3, for wild-type OBP the transition temperatures of odorants 3 and 4 featuring a vinylic side chain is comparable with eugenol, which is otherwise structurally analogous. For the mutant protein however, the transition temperatures of these odorants are significantly decreased. A possible explanation for the lower odorant affinity of mutant OBP14 is the constricted flexibility introduced by the additional disulfide bond. Whereas the more flexible wild-type protein can adjust the shape of its binding cavity to form hydrophobic

interactions with the vinylic double bond, this adaptation is not possible for the mutant due to conformational restrictions. It has been reported that the binding cavity of OBP14 changes its size up to 20 % upon odorant binding [18], and that a certain degree of conformational flexibility is required for OBPs to properly interact with odorants [52]. The equivalently low change in transition temperatures of odorants 2 and 5 for both wild-type and mutant OBP14 may be explained by the dominating influence of the methoxy group as discussed above.

In homovanillic acid (6), coniferyl aldehyde (7) and coniferyl alcohol (8), the position 1 of the benzene ring possesses polar and charged groups in contrast to odorants 1-5 that feature hydrophobic side chains at this position. Evidently, a hydrophilic group is unfavourable at this site for both wild-type and mutant OBP14, because the affinities are significantly lower for these odorants (Fig. 3). This finding is experimental proof for the hypothesis stated in an earlier study that these polar groups have a negative effect on the interaction with the hydrophobic binding pocket of OBP14, despite the evidently similar structures of the involved odorants [17].

In summary, we have systematically investigated the affinities of phenolic odorants with varying side chains to wild-type and mutant OBP14 of the honey bee. CD measurements at elevated temperatures of the proteins in absence of odorants revealed a higher thermal stability of the mutant exhibiting an additional disulfide bond not present in the wild-type C-minus OBP14. This finding was corroborated by molecular dynamics simulations. Relative affinities of odorants have been estimated due to the extent of increased thermal stability of the protein-odorant complex. Our results indicate that eugenol exhibits the highest affinity to both, wild-type and mutant OBP14. Replacing the hydroxyl group with a methoxy group at position 4 of the benzene ring causes a decreased affinity to both forms of OBP14, whereas exchange of the allylic group with a vinylic side chain at the R_1 substituent leads to an exclusive decline of affinities to mutant OBP14. Differences in odorant affinity between the

wild-type and mutant are attributed to lower flexibility of the mutant due to the additional disulfide bond. Odorants featuring a polar or charged group at the R_1 position show very low affinities to both types of OBP14.

In our lab, studies of odorant affinities to wild-type OBP14 utilizing a graphene-based FET sensor confirmed the high affinity of eugenol [4]. However, in that investigation also odorants with a polar side chain show medium to high affinity. In the future, we intend to employ molecular dynamics simulations to explain this variance and to further explore the molecular basis of odorant affinities to OBPs.

Acknowledgements

Partial support for this work was provided by the European Science Foundation (ESF), the Austrian Science Fund (FWF) (I681-N24) and the Austrian Federal Ministry for Transport, Innovation and Technology (GZ BMVIT-612.166/0001-III/I1/2010).

Appendix A. Supplementary data

Supplementary data associated with this article can be found, in the online version, at http://dx.doi.org/10.1016/j.bbrc.

References

[1] K.C. Persaud, Biomimetic Olfactory Sensors, IEEE Sens. J. 12 (2012) 3108-3112.
[2] H.C. Lau, Y.K. Lee, J.Y. Kwon, Y.S. Sohn, J.O. Lim, LUSH-based SPR sensor for the detection of alcohols and pheromone, in: S.W. Kang, S.H. Park, L.P. Lee, K.B. Song, Y.H. Choi (Eds.), Nano-Bio Sensing, Imaging, and Spectroscopy, Spie-Int Soc Optical Engineering, Bellingham, 2013.
[3] Y. Lu, H. Li, S. Zhuang, D. Zhang, Q. Zhang, J. Zhou, S. Dong, Q. Liu, P. Wang, Olfactory biosensor using odorant-binding proteins from honeybee: Ligands of floral odors and pheromones detection by electrochemical impedance, Sens. Actuator B-Chem. 193 (2014) 420-427.
[4] M. Larisika, C. Kotlowski, C. Steininger, R. Mastrogiacomo, P. Pelosi, C. Kleber, W. Knoll, C. Nowak, Olfactory biosensor based on odorant binding protein 14 from

honeybee: Kinetic analysis of protein-ligand interaction, Biosens. Bioelectron. (2014) submitted.
[5] S. Sankaran, S. Panigrahi, S. Mallik, Odorant binding protein based biomimetic sensors for detection of alcohols associated with Salmonella contamination in packaged beef, Biosens. Bioelectron. 26 (2011) 3103-3109.
[6] F. Di Pietrantonio, D. Cannata, M. Benetti, E. Verona, A. Varriale, M. Staiano, S. D'Auria, Detection of odorant molecules via surface acoustic wave biosensor array based on odorant-binding proteins, Biosens. Bioelectron. 41 (2013) 328-334.
[7] S. Capone, C. Pascali, L. Francioso, P. Siciliano, K.C. Persaud, A.M. Pisanelli, Odorant Binding Proteins as Sensing Layers for Novel Gas Biosensors: An Impedance Spectroscopy Characterization, in: G. Neri, N. Donato, A. d'Amico, C. Di Natale (Eds.), Sensors and Microsystems, Springer Netherlands, 2011, pp. 317-324.
[8] S. Sankaran, L.R. Khot, S. Panigrahi, Biology and applications of olfactory sensing system: A review, Sens. Actuator B-Chem. 171 (2012) 1-17.
[9] S.H. Lee, H.J. Jin, H.S. Song, S. Hong, T.H. Park, Bioelectronic nose with high sensitivity and selectivity using chemically functionalized carbon nanotube combined with human olfactory receptor, J. Biotechnol. 157 (2012) 467-472.
[10] H.J. Jin, S.H. Lee, T.H. Kim, J. Park, H.S. Song, T.H. Park, S. Hong, Nanovesicle-based bioelectronic nose platform mimicking human olfactory signal transduction, Biosens. Bioelectron. 35 (2012) 335-341.
[11] P. Pelosi, Odorant-Binding Proteins, Crit. Rev. Biochem. Mol. 29 (1994) 199-228.
[12] J.J. Zhou, Odorant-binding proteins in insects, in: G. Litwack (Ed.), Vitamins and Hormones: Pheromones, Elsevier Academic Press Inc, San Diego, 2010, pp. 241-272.
[13] R.G. Vogt, R. Rybczynski, M.R. Lerner, Molecular-Cloning and Sequencing of General Odorant Binding-Proteins Gobp1 and Gobp2 from the Tobacco Hawk Moth Manduca-Sexta - Comparisons with Other Insect Obps and Their Signal Peptides, J. Neurosci. 11 (1991) 2972-2984.
[14] W.S. Leal, Odorant reception in insects: roles of receptors, binding proteins, and degrading enzymes, Annu. Rev. Entomol. 58 (2013) 373-391.
[15] H.G.S. Consortium, Insights into social insects from the genome of the honeybee Apis mellifera, Nature 443 (2006) 931-949.
[16] S. Foret, R. Maleszka, Function and evolution of a gene family encoding odorant binding-like proteins in a social insect, the honey bee (Apis mellifera), Genome Res. 16 (2006) 1404-1413.
[17] I. Iovinella, F.R. Dani, A. Niccolini, S. Sagona, E. Michelucci, A. Gazzano, S. Turillazzi, A. Felicioli, P. Pelosi, Differential expression of odorant-binding proteins in the mandibular glands of the honey bee according to caste and age, J. Proteome Res. 10 (2011) 3439-3449.
[18] S. Spinelli, A. Lagarde, I. Iovinella, P. Legrand, M. Tegoni, P. Pelosi, C. Cambillau, Crystal structure of Apis mellifera OBP14, a C-minus odorant-binding protein, and its complexes with odorant molecules, Insect Biochem. Mol. Biol. 42 (2012) 41-50.
[19] L.P. Ban, L. Zhang, Y.H. Yan, P. Pelosi, Binding properties of a locust's chemosensory protein, Biochem. Biophys. Res. Commun. 293 (2002) 50-54.
[20] M. Wogulis, T. Morgan, Y. Ishida, W.S. Leal, D.K. Wilson, The crystal structure of an odorant binding protein from Anopheles gambiae: Evidence for a common ligand release mechanism, Biochem. Biophys. Res. Commun. 339 (2006) 157-164.
[21] F.F. Damberger, E. Michel, Y. Ishida, W.S. Leal, K. Wüthrich, Pheromone discrimination by a pH-tuned polymorphism of the Bombyx mori pheromone-binding protein, Proc. Natl. Acad. Sci. (2013).

[22] F. Yu, S. Zhang, L. Zhang, P. Pelosi, Intriguing similarities between two novel odorant-binding proteins of locusts, Biochem. Biophys. Res. Commun. 385 (2009) 369-374.
[23] L. Ban, E. Napolitano, A. Serra, X. Zhou, I. Iovinella, P. Pelosi, Identification of pheromone-like compounds in male reproductive organs of the oriental locust Locusta migratoria, Biochem. Biophys. Res. Commun. 437 (2013) 620-624.
[24] A. Schwaighofer, C. Kotlowski, C. Araman, N. Chu, R. Mastrogiacomo, C. Becker, P. Pelosi, W. Knoll, M. Larisika, C. Nowak, Honey bee odorant-binding protein 14: effects on thermal stability upon odorant binding revealed by FT-IR spectroscopy and CD measurements, Eur. Biophys. J. (2013).
[25] S.M. Kelly, T.J. Jess, N.C. Price, How to study proteins by circular dichroism, Biochim. Biophys. Acta, Proteins Proteomics 1751 (2005) 119-139.
[26] M.S. Celej, S.A. Dassie, E. Freire, M.L. Bianconi, G.D. Fidelio, Ligand-induced thermostability in proteins: thermodynamic analysis of ANS-albumin interaction, Biochim. Biophys. Acta 1750 (2005) 122-133.
[27] M.J. Moreau, I. Morin, P.M. Schaeffer, Quantitative determination of protein stability and ligand binding using a green fluorescent protein reporter system, Mol. Biosyst. 6 (2010) 1285-1292.
[28] M.S. Celej, G.G. Montich, G.D. Fidelio, Protein stability induced by ligand binding correlates with changes in protein flexibility, Protein. Sci. 12 (2003) 1496-1506.
[29] D.H. Williams, E. Stephens, D.P. O'Brien, M. Zhou, Understanding Noncovalent Interactions: Ligand Binding Energy and Catalytic Efficiency from Ligand-Induced Reductions in Motion within Receptors and Enzymes, Angew. Chem., Int. Ed. 43 (2004) 6596-6616.
[30] O.V. Stepanenko, A. Marabotti, I.M. Kuznetsova, K.K. Turoverov, C. Fini, A. Varriale, M. Staiano, M. Rossi, S. D'Auria, Hydrophobic interactions and ionic networks play an important role in thermal stability and denaturation mechanism of the porcine odorant-binding protein, Proteins: Struct., Funct., Genet. 71 (2008) 35-44.
[31] S. Kumar, C.-J. Tsai, R. Nussinov, Factors enhancing protein thermostability, Protein Eng. 13 (2000) 179-191.
[32] S. Katada, T. Hirokawa, Y. Oka, M. Suwa, K. Touhara, Structural basis for a broad but selective ligand spectrum of a mouse olfactory receptor: mapping the odorant-binding site, J. Neurosci. 25 (2005) 1806-1815.
[33] O. Baud, S. Etter, M. Spreafico, L. Bordoli, T. Schwede, H. Vogel, H. Pick, The Mouse Eugenol Odorant Receptor: Structural and Functional Plasticity of a Broadly Tuned Odorant Binding Pocket, Biochemistry 50 (2011) 843-853.
[34] K.H. Tan, R. Nishida, Methyl Eugenol: Its Occurrence, Distribution, and Role in Nature, Especially in Relation to Insect Behavior and Pollination, J. Insect Sci. 12 (2012) 1-60.
[35] F.R. Dani, I. Iovinella, A. Felicioli, A. Niccolini, M.A. Calvello, M.G. Carucci, H.L. Qiao, G. Pieraccini, S. Turillazzi, G. Moneti, P. Pelosi, Mapping the Expression of Soluble Olfactory Proteins in the Honeybee, J. Proteome Res. 9 (2010) 1822-1833.
[36] L. Ban, A. Scaloni, A. Brandazza, S. Angeli, L. Zhang, Y. Yan, P. Pelosi, Chemosensory proteins of Locusta migratoria, Insect Mol. Biol. 12 (2003) 125-134.
[37] M. Calvello, N. Guerra, A. Brandazza, C. D'Ambrosio, A. Scaloni, F.R. Dani, S. Turillazzi, P. Pelosi, Soluble proteins of chemical communication in the social wasp Polistes dominulus, Cell. Mol. Life Sci. 60 (2003) 1933-1943.
[38] N. Schmid, C.D. Christ, M. Christen, A.P. Eichenberger, W.F. van Gunsteren, Architecture, implementation and parallelisation of the GROMOS software for biomolecular simulation, Comput. Phys. Commun. 183 (2012) 890-903.

[39] M.M. Reif, P.H. Hunenberger, C. Oostenbrink, New Interaction Parameters for Charged Amino Acid Side Chains in the GROMOS Force Field, J. Chem. Theory Comput. 8 (2012) 3705-3723.
[40] L. Briand, N. Swasdipan, C. Nespoulous, V. Bézirard, F. Blon, J.-C. Huet, P. Ebert, J.-C. Pernollet, Characterization of a chemosensory protein (ASP3c) from honeybee (Apis melliferaL.) as a brood pheromone carrier, Eur. J. Biochem. 269 (2002) 4586-4596.
[41] S.M. Kelly, N.C. Price, The Use of Circular Dichroism in the Investigation of Protein Structure and Function, Curr. Protein Pept. Sci. 1 (2000) 349-384.
[42] M. Staiano, S. D'Auria, A. Varriale, M. Rossi, A. Marabotti, C. Fini, O.V. Stepanenko, I.M. Kuznetsova, K.K. Turoverov, Stability and dynamics of the porcine odorant-binding protein, Biochemistry 46 (2007) 11120-11127.
[43] P. Pelosi, R. Mastrogiacomo, I. Iovinella, E. Tuccori, K.C. Persaud, Structure and biotechnological applications of odorant-binding proteins, Appl. Microbiol. Biotechnol. 98 (2014) 61-70.
[44] C.N. Pace, G.R. Grimsley, J.A. Thomson, B.J. Barnett, Conformational Stability and Activity of Ribonuclease-T1 with Zero, One, and 2 Intact Disulfide Bonds, J. Biol. Chem. 263 (1988) 11820-11825.
[45] Y. Li, P.M. Coutinho, C. Ford, Effect on thermostability and catalytic activity of introducing disulfide bonds into Aspergillus awamori glucoamylase, Protein Eng. 11 (1998) 661-667.
[46] M. Ramazzotti, C. Parrini, M. Stefani, G. Manao, D. Degl'Innocenti, The intrachain disulfide bridge is responsible of the unusual stability properties of novel acylphosphatase from Escherichia coli, FEBS Lett. 580 (2006) 6763-6768.
[47] D. Fass, Disulfide Bonding in Protein Biophysics, Annu. Rev. Biophys. 41 (2012) 63-79.
[48] M. Luckey, R. Ling, A. Dose, B. Malloy, Role of a disulfide bond in the thermal stability of the LamB protein trimer in Escherichia coli outer membrane, J. Biol. Chem. 266 (1991) 1866-1871.
[49] M. Parisi, A. Mazzini, R. Tibor Sorbi, R. Ramoni, S. Grolli, R. Favilla, Role of the disulphide bridge in folding, stability and function of porcine odorant binding protein: Spectroscopic equilibrium studies on C63A/C155A double mutant, Biochim. Biophys. Acta, Proteins Proteomics 1750 (2005) 30-39.
[50] A. Scire, A. Marabotti, M. Staiano, L. Briand, A. Varriale, E. Bertoli, F. Tanfani, S. DAuria, Structure and Stability of a Rat Odorant-Binding Protein: Another Brick in the Wall, J. Proteome Res. 8 (2009) 4005-4013.
[51] S. Paolini, F. Tanfani, C. Fini, E. Bertoli, P. Paolo, Porcine odorant-binding protein: structural stability and ligand affinities measured by Fourier-transform infrared spectroscopy and fluorescence spectroscopy, Biochim. Biophys. Acta, Protein Struct. Mol. Enzymol. 1431 (1999) 179-188.
[52] B.P. Ziemba, E.J. Murphy, H.T. Edlin, D.N.M. Jones, A novel mechanism of ligand binding and release in the odorant binding protein 20 from the malaria mosquito Anopheles gambiae, Protein Science 22 (2013) 11-21.

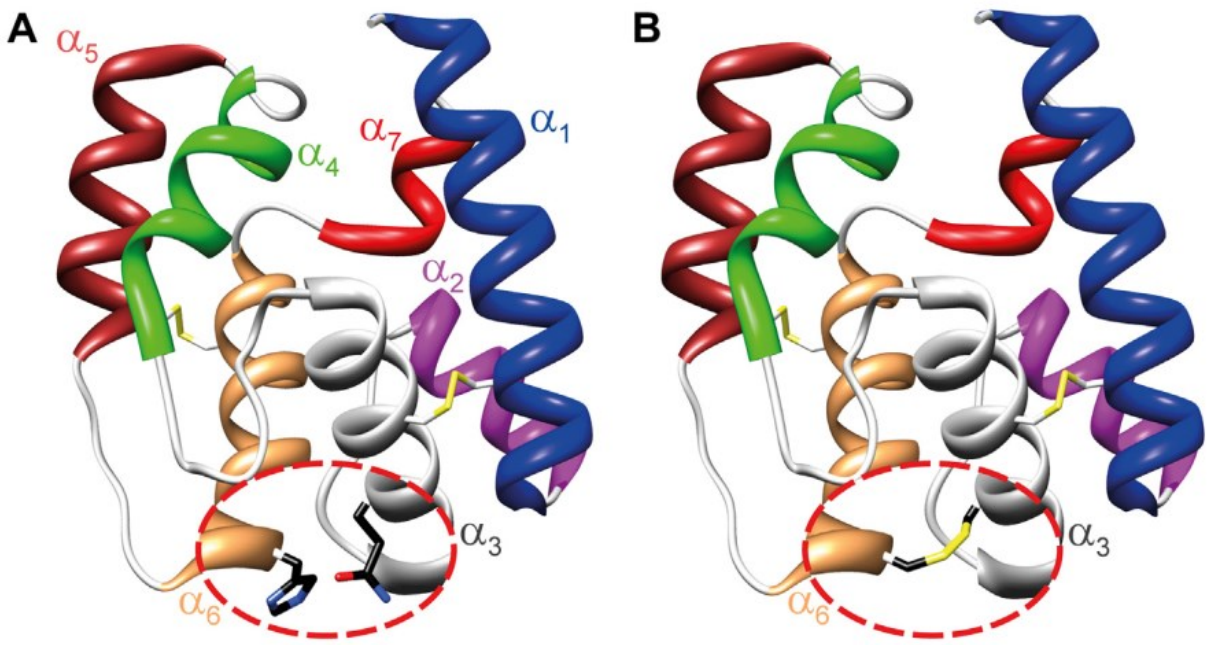

Fig. 1. Three dimensional model of (A) wild-type OBP14 and (B) mutant OBP14 featuring an additional disulfide bond between α3 and α6. OBP14 natively possesses two disulfide bonds between α1-α3 and α5-α6, respectively, thus being classified as a C-minus OBP.

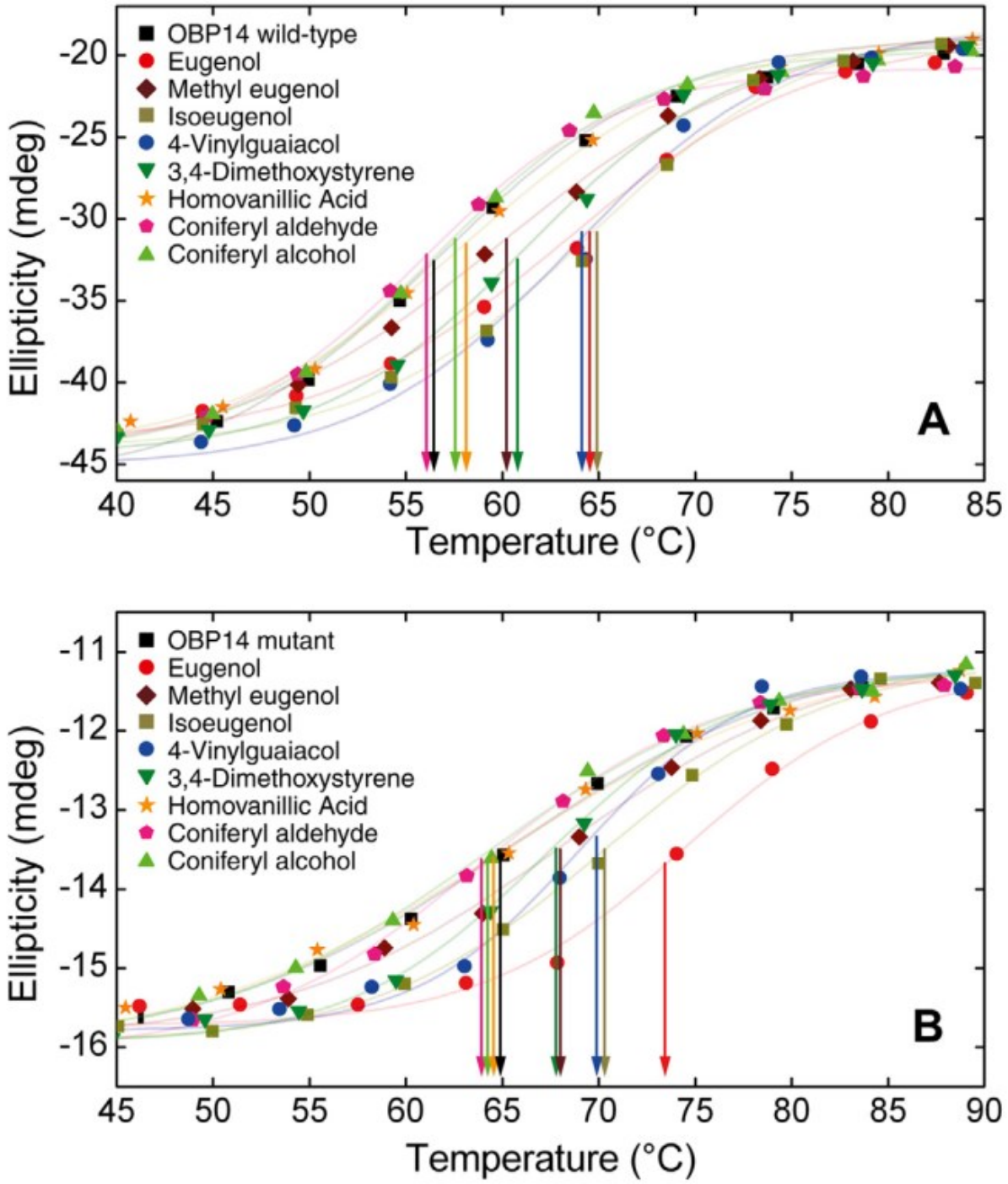

Fig. 2. Ellipticity at a wavelength of 222 nm of (A) wild-type and (B) mutant OBP14 in the absence and presence of odorants (data points). Lines indicate a Boltzmann fit for sigmoidal line shapes.

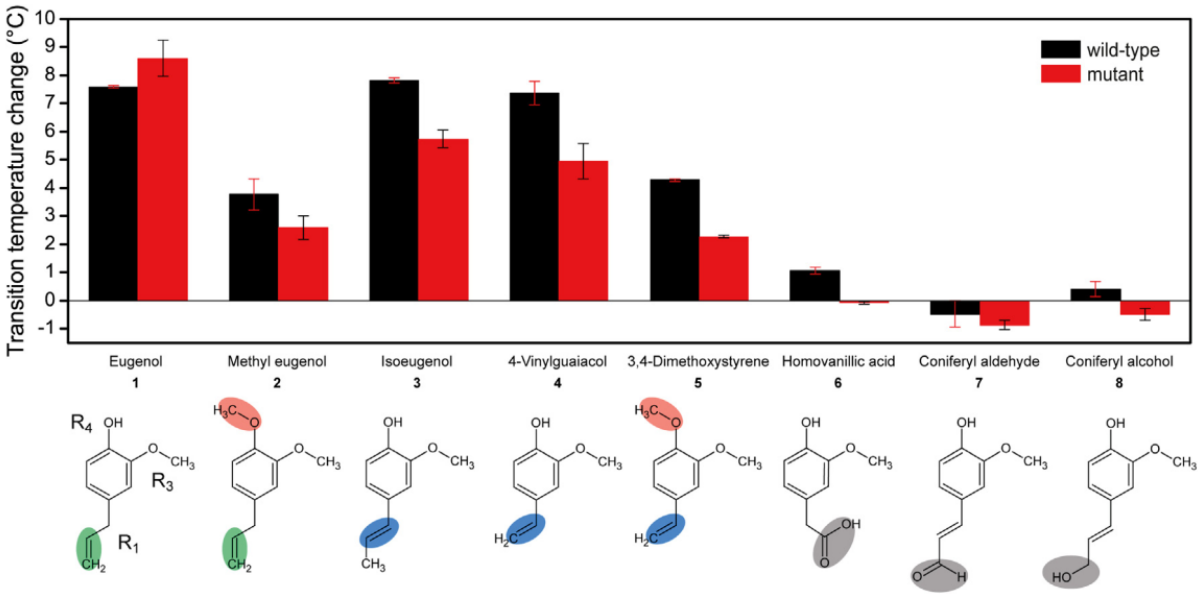

Fig. 3. Change in transition temperatures of the protein-odorant complexes of wild-type (black) and mutant (red) OBP14 relative to the transition temperature of the proteins in absence of odorants. Error bars indicate the standard deviation. Substituent R_3 contains a methoxy group for all odorants. At R_4, there is either a hydroxyl group or a methoxy group, whereas the R_1 position varies between hydrophobic and hydrophilic side groups.